



# Chapter 11

## Monitoring Memory B Cells by Next-Generation ImmunoSpot<sup>®</sup> Provides Insights into Humoral Immunity that Measurements of Circulating Antibodies Do Not Reveal

Paul V. Lehmann, Zhigang Liu, Noémi Becza, Alexis V. Valente, Junbo Wang, and Greg A. Kirchenbaum

### Abstract

Memory B cells ( $B_{\text{mem}}$ ) provide the second wall of adaptive humoral host defense upon specific antigen rechallenge when the first wall, consisting of preformed antibodies originating from a preceding antibody response, fails. This is the case, as recently experienced with SARS-CoV-2 infections and previously with seasonal influenza, when levels of neutralizing antibodies decline or when variant viruses arise that evade such. While in these instances, reinfection can occur, in both scenarios, the rapid engagement of preexisting  $B_{\text{mem}}$  into the recall response can still confer immune protection.  $B_{\text{mem}}$  are known to play a critical role in host defense, yet their assessment has not become part of the standard immune monitoring repertoire. Here we describe a new generation of B cell ELISPOT/FluoroSpot (collectively ImmunoSpot<sup>®</sup>) approaches suited to dissect, at single-cell resolution, the  $B_{\text{mem}}$  repertoire *ex vivo*, revealing its immunoglobulin class/subclass utilization, and its affinity distribution for the original, and for variant viruses/antigens. Because such comprehensive B cell ImmunoSpot<sup>®</sup> tests can be performed with minimal cell material, are scalable, and robust, they promise to be well-suited for routine immune monitoring.

**Key words** ELISPOT, FluoroSpot, B cells, Immune monitoring, Antibodies, Antibody titers, Immune memory, Affinity

---

## 1 Introduction

Clinical immune diagnostics are currently confined to the detection of specific antibodies in serum and other bodily fluids. Diagnostic decisions on whether a person has been infected by, and subsequently developed immunity, e.g., to a particular virus or vaccination, and the magnitude of the ensuing immune response are presently deduced from measurements of serum antibody titers. In this chapter, we will describe why it is necessary to include memory B cell ( $B_{\text{mem}}$ ) measurements into such considerations, and how this can be reliably accomplished with minimal cell

material and labor by performing B cell ELISPOT/FluoroSpot, collectively “ImmunoSpot<sup>®</sup>” assays (*see Note 1*).

There are conceptual and practical reasons why, thus far, mainstream efforts toward monitoring antigen-specific  $B_{\text{mem}}$  have not been sufficiently undertaken. Namely, it has largely been accepted that antibody titer measurements directly reflect  $B_{\text{mem}}$  frequencies. This notion has been based on the antiquated assumption that during the B cell response to antigen, long-lived  $B_{\text{mem}}$  and long-lived plasma cells (PC) arise in a fixed ratio to each other. Thus, the feeling had been that cumbersome assays to detect  $B_{\text{mem}}$  utilizing fragile live cell material are unnecessary because simple measurements of stable proteins in serum reliably provide the sought-after information. However, recent advances in the understanding of B cell lineage differentiation pathways imply the requirement for a different approach. This topic has been the subject of several excellent reviews recently [1–3] and is only outlined briefly in the following section.

### **1.1 Differential Fate Decisions for B Cell Differentiation into the Memory vs. Plasma Cell Lineages**

During the antigen-driven B cell response, within a germinal center (GC) present in the draining lymph node(s),  $B_{\text{mem}}$  and PC arise along differential, affinity-driven maturation pathways (Fig. 1). Briefly, when germinal center B cells (GCB) undergo proliferation and acquire somatic hypermutations (SHM) (*see Note 2*), daughter cells arise with mutated antigen-binding sites of their B cell antigen receptors (BCR) (*see Note 3*). Because SHM occurs somewhat randomly, a subset of these mutated BCR can acquire an increased affinity for the antigen, although the affinity of most BCR is either unaltered or attenuated as a result of these mutations. In subsequent steps, the progeny of GCB that gained an increased affinity for the antigen undergoes additional cycles of proliferation, SHM, and affinity-based positive selection. Multiple repetitions of this process eventually lead to the differentiation of PC, which constitutes the cellular basis of the affinity-matured antibody response. Progeny of GCB that do not meet the increasingly stringent antigen-driven affinity selection criterion (*see Note 4*) exit the GC and become long-lived  $B_{\text{mem}}$ .

$B_{\text{mem}}$  and PC, therefore, emerge along alternative routes driven by different selection criteria, and, subsequently, their frequencies are not necessarily linked. Consequently, one cannot expect antigen-specific serum antibody levels and  $B_{\text{mem}}$  frequencies to be proportional to each other. From the above understanding of antigen-driven B cell differentiation, it also follows that, while both PC and  $B_{\text{mem}}$  are antigen-specific (i.e., their BCR exceeds a minimal binding constant for antigen), PC (and hence secreted antibodies) constitute primarily the high affinity end of this affinity spectrum, while  $B_{\text{mem}}$  also encompass a lower affinity fraction. Recent interpretation of these findings even implies that PC and  $B_{\text{mem}}$  play fundamentally different roles in humoral immune defense [1].

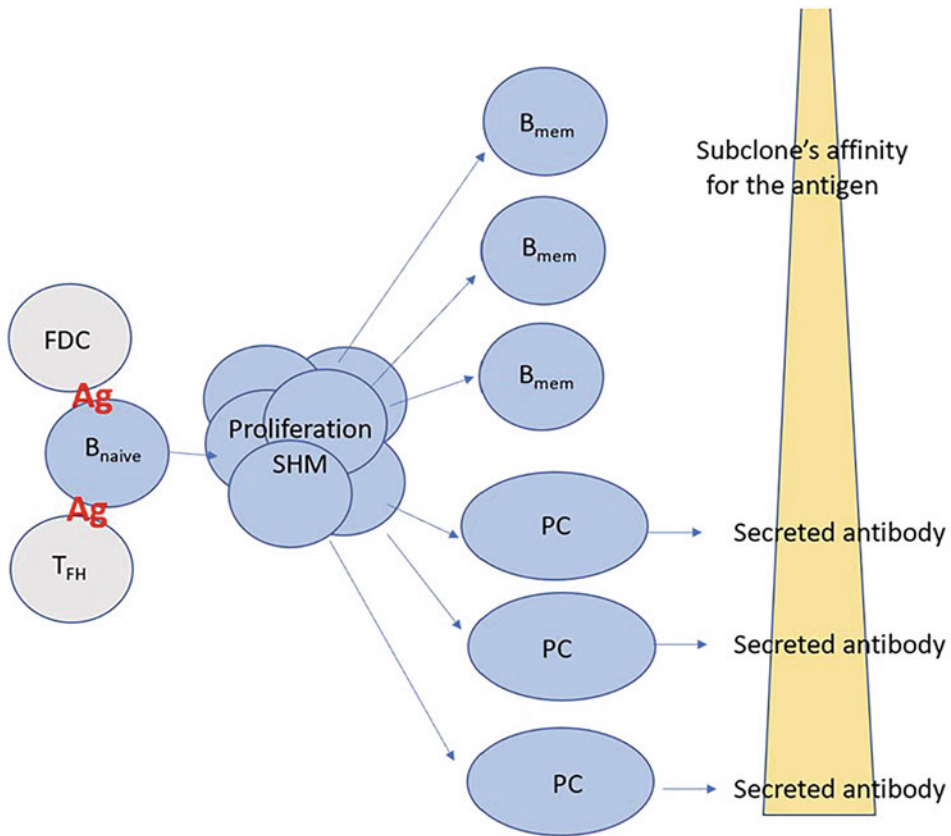


**Fig. 1** Affinity-based differential differentiation of plasma- and memory B cells. In a secondary lymphoid tissue, e.g., a lymph node, a naive B cell ( $B_{naive}$ ) encounters the homotypic antigen presented by a follicular dendritic cell (FDC) for which its B cell receptor (BCR) has sufficient affinity to trigger activation. The B cell then presents BCR-acquired antigen-derived peptides to cognate T follicular helper ( $T_{FH}$ ) cells, resulting in the activation/polarization and proliferation of both cell types. The B cell then enters a germinal center within the lymph node, where it undergoes additional rounds of proliferation and somatic hypermutation (SHM) of its BCR. Because the latter is random, the daughter cells display BCR with a broad spectrum of affinities for the homotypic antigen. Cells endowed with high-affinity BCR for the homotypic antigen are positively selected and undergo additional cycles of proliferation, acquisition of further somatic hypermutations, and affinity-based positive selection, eventually differentiating into antibody-secreting plasma cells (PC). Daughter cells that express lower affinity BCR variants for the homotypic antigen exit the lymph node as memory B cells ( $B_{mem}$ ). By chance cross-reactivity, however, some of these  $B_{mem}$  will have high affinity for heterotypic antigen variants

### 1.2 Serum Antibodies Reflect the First Wall of Adaptive Humoral Defense, $B_{mem}$ the Second

While PC elicited during the primary immune response can secrete large amounts of antibodies, their lifespans are heterogenous and, contrary to the previous assumption that PC are long-lived, likely fall on a continuum with possibly only a fraction of them surviving long-term [4, 5]. The antibody molecules they secrete are also relatively short-lived in the body and possess half-lives of several weeks, at best (*see* **Note 5**). Thus, serum antibodies that are

detected at any one time have been recently produced and, therefore, the maintenance of serum antibody levels depends on constant active replenishment by PC. Such antibodies in bodily fluids and their cell-bound variants (*see* **Notes 5–7**) constitute the first wall of the adaptive humoral immune defense since they are already present prior to antigen reencounter. Such antibodies (IgA and IgM) are transported across the mucosa and can confer instant host protection by preventing entry of the pathogen/antigen into the body. If the offending pathogen/antigen succeeds in crossing this interface and gains access into the body, preformed antibodies (IgG and IgM) already present in serum can still confer protection through direct neutralization. Serum antibodies also possess precipitating, opsonizing, and complement activating activity to further combat the dissemination of the pathogen/antigen. Preformed antibodies can additionally initiate inflammatory reactions through their interactions with Ig-binding receptors expressed on various immune cell populations (IgE, IgG, or IgM).

Many times, however, the first wall of adaptive humoral immune defense fails to prevent reinfection. Such is the case when antibody levels either decline to sub-protective levels, or when antigenic viral variants are encountered that evade neutralization, as evidenced, e.g., in the recent COVID pandemic. Boosting the levels of specific antibodies that were already established through infection or vaccination against the previously circulating virus strain, the “homotype,” will not confer sterilizing immunity against a newly emerging antigenic variant strain, the “heterotype.” In this case,  $B_{\text{mem}}$  provide the second wall of adaptive humoral immune defense. Within the  $B_{\text{mem}}$  pool established during a preceding immune response, BCR specificities possessing a reduced affinity for the homotypic virus/antigen will be present that, by chance, have an increased affinity for the variant, heterotypic virus/antigen. As such, heterotypic antigen-reactive  $B_{\text{mem}}$  occur at higher frequencies than would occur within a B cell repertoire that is naive to the homotypic virus/antigen; moreover, as such  $B_{\text{mem}}$  have already undergone immunoglobulin (Ig) class switch recombination (CSR), they can readily engage into faster and more efficient recall responses, including potential reentry into a GC for acquisition of further affinity-enhancing SHM. While this  $B_{\text{mem}}$ -based second wall of adaptive humoral immunity is not able to prevent infection with a heterotypic virus, it still mediates immune protection against it by enabling the host to rapidly mount a secondary-type immune response at the first encounter with a heterotypic virus.

Studying antigen-specific serum antibodies vs.  $B_{\text{mem}}$ , therefore, provides fundamentally different information on adaptive humoral immunity. The former reflects only on the past remnants of previously established, still deployable, but passive, and fading

immunological memory. In contrast, studies of  $B_{\text{mem}}$  provide insights into the ability of an individual to actively mount secondary immune responses against homo- and/or heterotypic antigens. Thus, studying  $B_{\text{mem}}$  permits one to take a glance into the future.

**1.3 Emerging Evidence for Serum Antibody Levels and Memory Cell Frequencies Providing Divergent Information on the Magnitude of B Cell-Mediated Immunity**

Recently, we concluded a systematic study (to the best of our knowledge the first on this subject) in which we measured circulating antibody levels to SARS-CoV-2, EBV, and different seasonal influenza virus strains and compared them with the frequencies of  $B_{\text{mem}}$  reactive with the same antigens [6]. These ImmunoSpot<sup>®</sup>-based  $B_{\text{mem}}$  detections were enabled by our newly acquired ability to achieve high-density antigen coating, thus reliable detection of  $B_{\text{mem}}$  specific for essentially any antigen ([11] and *see Note 8*). Representative results for the SARS-CoV-2 Spike protein are shown in Fig. 2. Notably, elevated frequencies of Spike-specific,  $B_{\text{mem}}$ -derived antibody-secreting cells (ASC) were detected in all of these convalescent COVID-19 donors despite variable levels of IgG antibody reactivity in the plasma at the time of sample collection. In

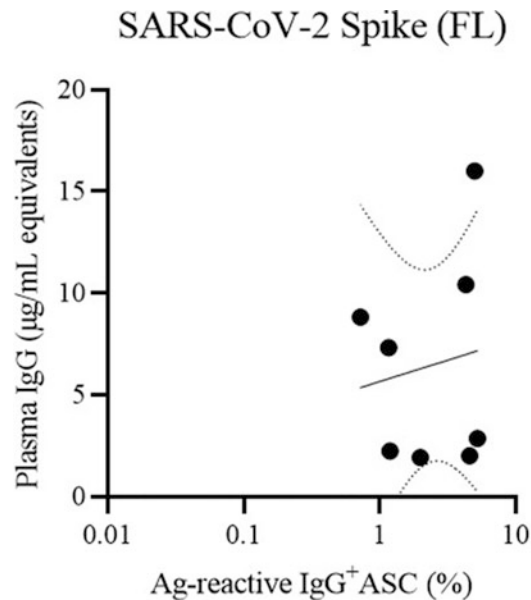


**Fig. 2** Discordance between circulating antibody levels and  $B_{\text{mem}}$  frequencies in PBMC against SARS-CoV-2 Spike antigen. Correlation between SARS-CoV-2 Spike (FL = full length)-specific IgG<sup>+</sup> antibody-secreting cell (ASC) frequencies (x-axis) and plasma IgG levels (y-axis) in convalescent COVID-19 donors ( $n = 8$ ). Pearson correlation analysis was performed using GraphPad Prism software on log-transformed antigen-specific ASC data and the corresponding antigen-specific IgG titers (expressed as µg/mL of IgG equivalents). Regression analysis was also performed using GraphPad Prism and the 95% confidence bands are plotted. These data are representative of similar findings reported previously for this and other viral antigens [6]

this same study [6], discordance between antibody levels and  $B_{\text{mem}}$ -derived ASC frequencies was also noted for the SARS-CoV-2 NCAP antigen and multiple antigenically unrelated seasonal influenza strains, all of which represent respiratory viruses that cause acute, short-term infections. Furthermore, discordance between antibody levels and  $B_{\text{mem}}$ -derived ASC frequencies was also evidenced against the EBNA1 antigen of Epstein–Barr virus (EBV), a latent herpesvirus that occasionally reactivates [7].

**1.4 Emerging Evidence for  $B_{\text{mem}}$  Detection Being More Reliable for Revealing Past Antigen Exposure than Serum Antibody Measurements**

It is not uncommon to find individuals who exhibit little if any seropositivity for an antigen, yet possess significant, often high, frequencies of antigen-specific,  $B_{\text{mem}}$ -derived ASC (Fig. 2, [6], and Kirchenbaum et al., manuscript in preparation). Among the antigens tested, SARS-CoV-2 proteins are the most informative in this regard because SARS-CoV-2 Spike and NCAP antigen-specific  $B_{\text{mem}}$ -derived ASC are not detected in samples from individuals cryopreserved prior to the onset of the COVID-19 pandemic (which, therefore, are verifiably immunologically naive to this virus owing to the time period in which these samples were collected). In contrast, each of the seronegative, yet  $B_{\text{mem}}$ -positive, donors in our study cohort had undergone PCR-verified SARS-CoV-2 infections (*see Note 9*). In these instances, serum antibody measurements provided clearly false-negative results on the infection history of these individuals, while the presence of  $B_{\text{mem}}$ -derived ASC reliably revealed it.

We have also previously noted clearly false-negative serological assessments for human cytomegalovirus (HCMV) exposure [8]. Obtaining PBMC (peripheral blood mononuclear cells) from different FDA-approved blood banks, all of which screen their donors for HCMV seropositivity, we found that PBMC from many such HCMV-seronegative donors possessed HCMV antigen-reactive,  $B_{\text{mem}}$ -derived ASC in ImmunoSpot<sup>®</sup> assays following *in vitro* polyclonal stimulation. Such subjects also exhibited  $CD4^+$  and  $CD8^+$  T cell memory to HCMV. Thus, the presence of  $B_{\text{mem}}$ -derived ASC reactivity (and T cell memory) more reliably revealed the HCMV-exposed status of these donors than did serum antibody levels.

In yet another independent line of investigation, studying patients with multiple sclerosis (MS), an autoimmune disease of the central nervous system (CNS), we detected neuroantigen-specific  $B_{\text{mem}}$ , in the absence of detectable serum antibody levels in most patients, whereas such  $B_{\text{mem}}$  were absent in healthy controls [9]. Collectively these findings suggest that detecting  $B_{\text{mem}}$ -derived ASC might be a more reliable way to diagnose past infections and possibly also autoimmune diseases than afforded presently by serum antibody measurements.

**1.5 Assessing  $B_{mem}$  Might Be Important, but how, and why?**

Presently there are two major techniques that permit the detection of antigen-specific  $B_{mem}$  in blood, lymphoid tissues, and other primary cell material. One approach is based on labeling B cells with fluorescently tagged antigen(s) followed by their detection using flow cytometry; the other is by ImmunoSpot<sup>®</sup>. While the strength of the former approach is that it allows for the segregation of antigen probe-binding B cells into phenotypically distinct subsets based on their surface marker expression, it has several disadvantages compared to ImmunoSpot<sup>®</sup>. One crucial difference is the lower limit of detection of the former. While ImmunoSpot<sup>®</sup> enables measurement of a single ASC within a bulk population of cells with essentially no intrinsic lower detection limit (*see Note 10*), flow cytometry falls short of detecting antigen-specific B cells when they are present as low-frequency events.  $B_{mem}$ , however, frequently occurs in very low frequencies in PBMC (Fig. 3). Additionally, the number of PBMC required for flow cytometric detection of antigen-specific B cells is considerably higher compared to ImmunoSpot<sup>®</sup> (*see Note 11*). Notably, a surface staining-only approach for the identification of antigen-specific B cells does not reliably reveal the Ig class/subclass usage of ASC, while four-color ImmunoSpot<sup>®</sup> assays provide this key information with ease as part of routine  $B_{mem}$  frequency measurements (*see Note 12*). Lastly, unlike for flow cytometry, the actual wet lab implementation of B cell ImmunoSpot<sup>®</sup> assays is scalable for high-throughput analysis (*see Note 13*) and multi-color ImmunoSpot<sup>®</sup> analysis can be fully automated (*see Chap. 5 by Karulin et al. in this volume [10]*).

**1.6 Affinity Coating: Enabling B Cell ImmunoSpot<sup>®</sup> Assays “to See”**

With so many potential advantages in favor of ImmunoSpot<sup>®</sup> assays for the detection of  $B_{mem}$ , the question arises as to why this technique has not become more widely used for immune monitoring purposes. The answer is simple and practical: the original protocol (that involves direct coating of the antigen to the membrane) only works well for a rather limited set of antigens (*see Note 14*). Consequently, many investigators likely gave up on this assay after not being successful in their initial attempts to establish such assays for the antigen(s) of interest. Our recent introduction of affinity capture coating [11] represents a breakthrough to this end, as it provides a universal strategy for successful assay development for essentially any antigen: the membrane is first coated with an anti-(His- or other) affinity tag-specific antibody followed by the addition of recombinant (His- or other) affinity-tagged recombinant antigen. In this way, low-affinity absorption of the antigen to the membrane via weak, non-specific binding forces (primarily hydrophobicity) is replaced by specific, high-affinity binding. The assay principle is depicted in Fig. 4b, and the protocol is described in detail below. This version of the B cell ImmunoSpot<sup>®</sup> assay is

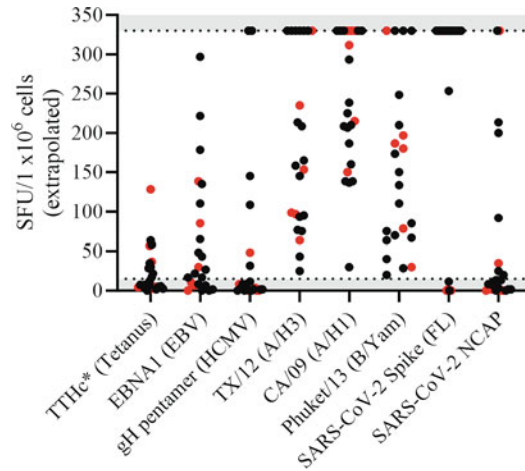


**Fig. 3** Antigen-specific  $B_{\text{mem}}$  occur over a wide frequency range in blood. PBMC from healthy human subjects – each represented by a dot – were tested via ImmunoSpot<sup>®</sup> assays to establish the frequency of  $\text{IgG}^+$   $B_{\text{mem}}$ -derived ASC specific for the panel of antigens shown: Tetanus toxoid heavy chain (TTHe), Epstein–Barr nuclear antigen (EBNA1) of EBV, gH pentamer complex (consisting of gH, gL, UL128, UL130, and UL131A proteins) of HCMV, recombinant hemagglutinin (rHA) proteins representative of A/California/2009 (H1N1), A/Texas/2013 (H3N2), and B/Phuket/2013 (Yamagata lineage) seasonal influenza vaccine strains, as well as SARS-CoV-2 Spike (full-length) and Nucleocapsid (NCAP) proteins. Serving as specificity controls for SARS-CoV-2 antigens, donors whose PBMC were cryopreserved prior to widespread COVID infection and vaccination (before June 2021) are depicted as red dots, and subjects whose PBMC were frozen after June 2021 are denoted as black dots. Note, the data shown are results of testing PBMC without serial dilution at a fixed input of  $3 \times 10^5$  PBMC per well, and because quantification in wells with  $>100$  antigen-specific spot-forming units (SFU) is no longer precise, we defined the upper limit for accurate counts at 330 SFU per  $10^6$  PBMC. Values exceeding this threshold, denoted by the gray shading in the figure, require lower cell inputs for accurate quantification of antigen-specific ASC frequencies. Likewise, the lower gray-shaded region denotes low-frequency responses in which Poisson noise necessitates seeding higher PBMC numbers per well and larger numbers of replicate wells to be evaluated for accurate determination of antigen-specific ASC frequencies (*see Note 10*)

particularly well-suited for detecting and characterizing rare antigen-specific,  $B_{\text{mem}}$ -derived ASC in a test sample, whereas an alternative variant of the B cell ImmunoSpot<sup>®</sup> assay approach, which enables assessment of ASC functional affinity and is described in another chapter of this volume [12], is better suited for samples in which antigen-specific ASC are present at an elevated frequency among all ASC (*see Note 15*).



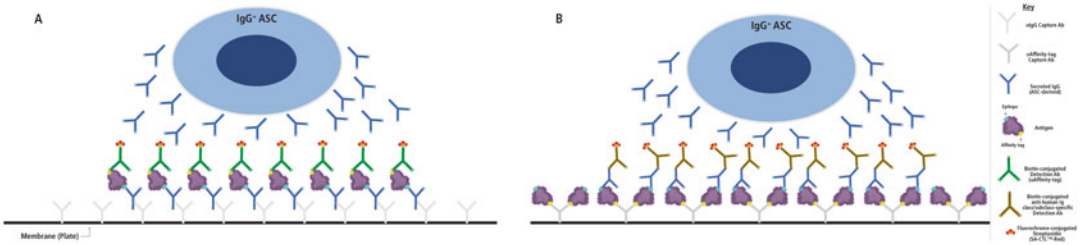


**Fig. 4** Principle of antigen-specific, **(a)** inverted vs. **(b)** direct B cell ImmunoSpot<sup>®</sup> assays (the latter, using the affinity capture coating approach). In **(a)**, the PVDF membrane on the bottom of a 96-well plate is densely coated with a pan anti-Ig(G) class-specific (in this example IgG) capture antibody that will bind the ASC-secreted Ig(G) with high affinity irrespective of the ASC's antigen specificity. In **(b)**, the membrane is coated first with an anti-affinity tag-specific antibody (in this example anti-His) that captures the (His)-tagged antigen with high affinity. In this way, dense coating of the membrane with the antigen is accomplished. As the next step in both assay variants, the PBMC containing the ASC are plated. In **(a)**, ASC-produced IgG is captured around each ASC that is secreting IgG and results in the formation of individual secretory footprints. In **(b)**, only the antibody produced by antigen-specific ASC is captured on the lawn of antigen. After removal of the cells, **(a)** the affinity-tagged (in this example His) antigen is added at a sufficient concentration to be retained by antigen-specific secretory footprints generated by ASC producing low- or high-affinity antibody. Alternatively, after removal of cells, **(b)** antigen-bound antibody is visualized by biotinylated human Ig class/subclass- (in this example IgG) specific detection antibodies. In **(a)**, antigen-specific secretory footprints are then visualized using a biotinylated anti-affinity tag detection reagent, which is revealed by the addition of a fluorescently conjugated streptavidin (FluoroSpot, as shown) or via an enzymatic reaction (ELISPOT, not shown). In **(b)**, antigen-specific secretory footprints are revealed by the addition of a fluorescently conjugated streptavidin (FluoroSpot, as shown) or via an enzymatic reaction (ELISPOT, not shown). In both B cell ImmunoSpot<sup>®</sup> assays, counting the spot-forming units (SFU) per well reveals the number of antigen-specific ASC within the PBMC plated. Furthermore, spot morphologies in such antigen-specific ImmunoSpot<sup>®</sup> assays also provide insights into the functional affinities of the antibody secreted by the individual ASC for the antigen, a topic covered in detail in the chapter by Becza et al., in this issue [12]

### 1.7 High-Content Information Provided by Assessing Individual ASC via ImmunoSpot<sup>®</sup> vs. Serum Antibody Measurements

Owing to the single-cell resolution afforded by ImmunoSpot<sup>®</sup> assays, they are ideally suited to study individual ASC that comprise an antigen-specific B cell response. While traditional serum antibody measurement techniques readily perceive large increases in antigen-specific antibody titers, they fail to appreciate more subtle changes in antibody levels, especially when the abundance of antibodies is very small, e.g., in the context of allergen-specific IgE [13], or when an elevated level of preexisting antibody reactivity is already present, e.g., in the context of studying seasonal influenza vaccine responses [14, 15]. In contrast, B cell ImmunoSpot<sup>®</sup> assays circumvent ambiguity in both cases through quantifying the precise number of cells that are actively secreting antigen-specific antibody and thus offer increased sensitivity and resolution.

When optimal antigen-coating conditions exist in the direct B cell ImmunoSpot<sup>®</sup> assay, each secretory footprint will be composed of antibody originating from a single ASC and thus permits assessment of antibody affinity similar to that achieved through studying an individual monoclonal antibody (mAb). In this setup,

the morphology of an ASC-derived secretory footprint is primarily defined by the affinity of the secreted antibody for the membrane-bound antigen. In agreement with prior computational modeling [16], we routinely observe variable spot morphologies in such antigen-specific B cell ImmunoSpot<sup>®</sup> assays [6, 11]. Importantly, beyond enumeration of such antigen-specific secretory footprints, a multitude of morphological features including metrics of intensity and size are also captured for each spot-forming unit (SFU) and are readily exported as flow cytometry standard (FCS) files by the ImmunoSpot<sup>®</sup> software. Such FCS files can be leveraged to visualize variable spot morphology, as was done using scatter plots in our recent publications [6, 11]. Here, we direct the reader to Chap. 5 by Karulin et al. in this volume that is dedicated to high-content analysis of spot morphologies [10]. Additionally, in the context of an inverted B cell ImmunoSpot<sup>®</sup> assay (*see Note 16*) in which ASC-derived secretory footprints are efficiently captured irrespective of antigen specificity, secretory footprints originating from individual antigen-specific ASC are revealed by their ability to retain an antigen probe. While also briefly introduced below, Chap. 13 in this volume by Becza et al. [12] describes in detail how the inverted ImmunoSpot<sup>®</sup> assay variant and high-content data analysis enable assessment of the functional affinity distribution present in a polyclonal population of ASC, such as the ASC response elicited following COVID-19 vaccination.

**1.8 Frequency of Antigen-Specific, B<sub>mem</sub>-Derived ASC Reflect Memory Potential**

Because ImmunoSpot<sup>®</sup> assays detect the secretory footprints of individual ASC, frequency information is revealed by counting the numbers of antigen-specific SFU, either per cells plated per well, or, better, as the frequency of antigen-specific ASC secreting a given Ig class/subclass among all ASC producing that Ig class/subclass (*see Note 16*). In either case, however, the crowding of secretory footprints along with the ELISA effect (*see Note 17*) can lead to undercounting of secretory footprints [6]. Systematically studying this phenomenon previously, we found that there exists a range in which cell numbers plated per well are directly proportional to the number of SFU detected. Depending on the nature of the assay and morphology of the resulting SFU, however, the corresponding SFU counts measured at higher cell inputs may break down at approximately 100–200 SFU per well (*see Note 18*). This is a major concern for establishing accurate frequencies of antigen-specific, B<sub>mem</sub>-derived ASC, especially in light of our previous data demonstrating that frequencies may span orders of magnitude for the same antigen in different individuals (Fig. 2 and [6]). Also, within any single individual, the frequency of B<sub>mem</sub>-derived ASC specific for different antigens can span a similarly wide distribution [6]. Furthermore, even the number of ASC producing a given Ig class/subclass, irrespective of antigen specificity, exhibits considerable interindividual variation. ELISA effects in B cell

ImmunoSpot<sup>®</sup> assays can also jeopardize high-content analysis of spot morphologies. A simple and efficient solution to this problem is to serially dilute the cell input to establish the linear range of SFU counts from which the accurate frequency of ASC can be extrapolated by linear regression ([6] and *see Note 19*). Karulin et al., Chap. 5 in this volume [10], introduce software for automatically establishing frequencies from such serial dilution experiments making this approach suitable for high-throughput workflows.

### 1.9 Defining the Ig Class/Subclass Usage of Antigen-Specific $B_{mem}$

The different Ig classes and subclasses are endowed with distinct effector functions and each contributes nonredundant roles toward maintaining host defense (see above and reviewed in greater detail in [17]). During the primary immune response, B cells can transition from IgM-expressing naive B cells into effector cells (PC) and  $B_{mem}$  that have undergone class switch recombination (CSR) [1]. CSR is an irreversible process involving the excision of DNA encompassing the exons of the  $Ig\mu$  heavy chain required for expression of IgM and juxtaposition of the upstream variable region genes (VDJ; which jointly define the antigen specificity of the BCR or secreted antibody) with downstream exons encoding alternative Ig classes or IgG subclasses [18]. Class switching of the BCR to downstream Ig classes or IgG subclasses is an instructed process and can be influenced by the cytokine milieu and co-stimulation provided by  $CD4^+$  T helper cells. For the latter, the differentiation of naive  $CD4^+$  T cells into different T helper cell classes (Th1, Th2, Th17, etc.) is defined by the circumstances of antigen encounter, in particular by Toll-like receptor (TLR)-derived signals [19, 20]. Triggering the “appropriate” type of T helper cells capable of stimulating the optimal Ig class usage during an infection or following vaccination is vital to successful host defense and the avoidance of collateral immune-mediated pathology (reviewed in [21]). The same applies to reinfection with the same pathogen.

Upon antigen reencounter and subsequent reactivation,  $B_{mem}$  rapidly differentiates into PC that secrete the same Ig class/subclass expressed by the parental  $B_{mem}$ . Therefore, detecting the Ig class/subclass that  $B_{mem}$ -derived ASC produced in B cell ImmunoSpot<sup>®</sup> assays permits the prediction of the specific types of antibodies that will be produced following the next antigen encounter (*see Notes 20–22*). Learning about the full spectrum of Ig classes/subclasses that the antigen-specific  $B_{mem}$  repertoire will produce when the antigen is reencountered is thus essential for predicting the protective efficacy of future antibody responses to an antigen. Moreover, such B cell ImmunoSpot<sup>®</sup> assays may also predict the likelihood of antibody-mediated complications occurring upon antigen re-exposure (as illustrated by the example of antibody-dependent enhancement leading to exacerbation of clinical disease following secondary dengue infection [22]). Importantly, the frequency of antigen-specific  $B_{mem}$  capable of secreting different Ig classes or

IgG subclasses can be orders of magnitude apart [6] (and see also Yao et al., Chap. 15 in this volume [23]). Thus, it is not only recommended to assess all antigen-specific Ig classes/subclasses, but also to do so over a wide frequency range for each. The latter can be readily accomplished by combining the serial dilution strategy described above with four-color ImmunoSpot<sup>®</sup> analysis (for details, see the Chap. 15 of Yao et al. in this volume, [23]).

### **1.10 Assessing the Affinity Distribution of the Antigen-Specific B<sub>mem</sub> Repertoire**

As described above in this chapter, and briefly recapitulated here, SHM leads to the diversification of B<sub>mem</sub> cells that previously participated in a GC reaction [24]. Upon reencounter with the same (homo-) or a modified (heterotypic) antigen, previously generated B<sub>mem</sub> endowed with high-affinity BCR for the rechallenging antigen will readily differentiate into PC that are capable of rapidly increasing antibody titers [3]. Moreover, B<sub>mem</sub> can also be re-recruited into a GC following antigen reencounter, where they will undergo further rounds of proliferation and acquire additional SHM necessary to refine and improve their BCR affinity for the offending antigen. Again, the GCB cell progeny endowed with the highest affinity BCR for the eliciting antigen will be selected for PC differentiation and ideally will enter the potentially long-lived fraction of the PC compartment. Thus, a B<sub>mem</sub> repertoire that entails a higher frequency of high-affinity B cells specific for the (homo- or heterotypic) antigen can generate a faster and more robust anamnestic antibody response upon antigen (re)encounter.

Thus far, the study of BCR/antibody affinity for a particular antigen has largely been confined to the generation of B cell hybridomas and/or paired *IgH/IgL* sequencing followed by expression and purification of individual mAb in order to establish their specificities and affinity using surface plasmon resonance or biolayer interferometry. While these approaches are the gold standard for studying individual mAbs (i.e., single B cells), it would require generation and subsequent characterization of hundreds of such mAbs to appreciate the underlying affinity distribution of antigen-specific B<sub>mem</sub> repertoire in just one donor, at a single timepoint, and against only a single antigen of interest. While such an exercise is, in theory at least, conceptually possible for a very limited number of individuals, it would be inconceivable both in magnitude and cost to attempt such an objective for a larger donor cohort, e.g., as part of a clinical trial. Consequently, this traditional method for characterizing the affinity distribution of the antigen-specific B cell repertoire is not realizable for high-throughput immune monitoring efforts.

The Chap. 13 in this volume by Becza et al. [12] demonstrates that the affinity distribution information of the antigen-specific B cell repertoire can be established with ease, and in a readily scalable manner, using two B cell ImmunoSpot<sup>®</sup> assay variants. For both, to characterize the affinity distribution of, e.g., vaccine-

elicited IgG<sup>+</sup> ASC, a first experiment would need to be performed that establishes the frequency of such antigen-specific IgG<sup>+</sup> ASC using the serial dilution approach (*see* **Note 23**). This information is essential for being able to seed in a follow-up test the PBMC at a “Goldilocks” cell density in which the individual secretory footprints can be studied without interfering with each other. In this second experiment, using an independent aliquot of cryopreserved cell material, the donor PBMC are seeded at the so-called “Goldilocks number,” which is assay dependent and between 50 and 100 SFU per well. As each SFU represents the secretory footprint of an individual ASC, at 50 SFU per well, the secretory footprints of 50 distinct ASC would be assessed. Seeding additional replicate wells at this “Goldilocks number” would increase the number of antigen-specific IgG<sup>+</sup> ASC being characterized. We recommend to study a fixed number of  $\geq 300$  ASC for each antigen concentration as this number gives a considerable (and representative) sample size for assessment of the antigen-specific B<sub>mem</sub> repertoire elicited in a particular person, against an individual antigen, at the time of sample collection.

Leveraging the inverted ImmunoSpot<sup>®</sup> approach for B cell affinity distribution measurements, the soluble antigen probe is added in decreasing concentrations to the same number of replicate wells for each antigen concentration, whereby each well was previously seeded with a “Goldilocks number” of cells. At the highest antigen probe concentration, the secretory footprints of all antigen-specific ASC, high- and low-affinity alike, will be detected as SFU when the membrane-retained antigen probe is visualized. In wells containing decreasing concentrations of the antigen probe, however, only the secretory footprints originating from ASC that produced an antibody with high affinity for the antigen probe will retain an adequate amount for their eventual detection as SFU; B cells with an affinity lower than dictated by the actual antigen concentration go undetected, and the SFU counts will decrease by their number. Therefore, establishing the SFU counts across a range of antigen probe concentrations provides insights into the affinity distribution of the antigen-specific B cell repertoire.

The second B cell ImmunoSpot<sup>®</sup> assay variant suited for assessment of the affinity distribution present in a polyclonal antigen-specific ASC compartment relies on a direct assay in which the antigen-coating density is graded. Such assays (Fig. 4) inherently provide information on the affinity of the “monoclonal antibody” that each antigen-specific ASC secretes. Following the basic rules of antibody–antigen binding, ASC that produce high-affinity antibodies generate dense, bright, and tight (sharp and small) secretory footprints (“spots”), while ASC that produce antibodies with lower affinity yield secretory footprints that are fainter and more diffuse [16]. Coating the membrane with decreasing densities of antigen and monitoring the resulting changes in SFU number and

morphology, therefore, provides information regarding the affinity distribution of an antigen-specific ASC repertoire (*see Note 24*). The Chap. 13 by Becza et al. in this volume [12] lays out in detail both assay variants for B cell affinity measurements.

### **1.11 Measuring Cross-Reactivities of Individual $B_{\text{mem}}$ -Derived ASC**

As described above,  $B_{\text{mem}}$  also provides a “second wall of adaptive humoral immunity” against mutated antigens/viruses (heterotypic antigens) that evolved to evade neutralizing antibodies induced by the original (homotypic) virus/antigen. While the primary response leads to fine tailoring of the B cell repertoire directed against the homotypic antigen, including affinity maturation, among the variants created by random SHM,  $B_{\text{mem}}$  endowed with BCR possessing affinity for the heterotypic antigen will be present. Even if such  $B_{\text{mem}}$  would be rare, and even if their initial affinity would be modest, they still would occur in much higher frequencies compared to the naive B cell repertoire. Moreover, most of these  $B_{\text{mem}}$  have already undergone Ig class switching. Therefore, when such clonally expanded, semi-affinity matured, and class-switched, cross-reactive  $B_{\text{mem}}$  engage in a primary immune response against the heterotypic antigen, they can generate a more rapid and efficient antibody response compared to individuals who have not been previously immunized/infected (*see Note 25*). Measuring existing serum antibodies does not detect such cross-reactive  $B_{\text{mem}}$ , and thus does not provide predictive information about cross-reactive protection, whereas ImmunoSpot<sup>®</sup>-based assessments at the level of individual  $B_{\text{mem}}$ -derived ASC do.

There are two ways to measure  $B_{\text{mem}}$ -derived ASC cross-reactivity by ImmunoSpot<sup>®</sup>. For both, the appropriate cell input per well first needs to be defined, which will provide the “Goldilocks” SFU count for the homotypic antigen (between 50 and 100 SFU per well, see above). In the simple version of B cell cross-reactivity studies, a second experiment is performed, an inverted B cell assay, in which this Goldilocks input of PBMC for the particular donor is seeded into all wells. Setting up replicate wells permits to assess  $\geq 300$  individual ASC-derived secretory footprints in independent single-color ImmunoSpot<sup>®</sup> assays, comparing the numbers of SFU detected in all replicates for the homotypic antigen, vs. the cumulative SFU number in the same number of replicate wells detected using the heterotypic antigen probe. The ratio of these two numbers reveals the percentage of cross-reactive ASC at equimolar concentrations of the respective antigen probes (*see Note 26* and Fig. 5). Raising/lowering the concentration of heterotypic antigen probe enables assessment of the affinity spectrum of  $B_{\text{mem}}$ -derived ASC that cross-react with the heterotypic antigen.

In a second, somewhat more complex but perhaps more elegant, approach,  $B_{\text{mem}}$ -derived ASC cross-reactivity is evaluated using alternatively labeled homotypic and heterotypic antigens. As

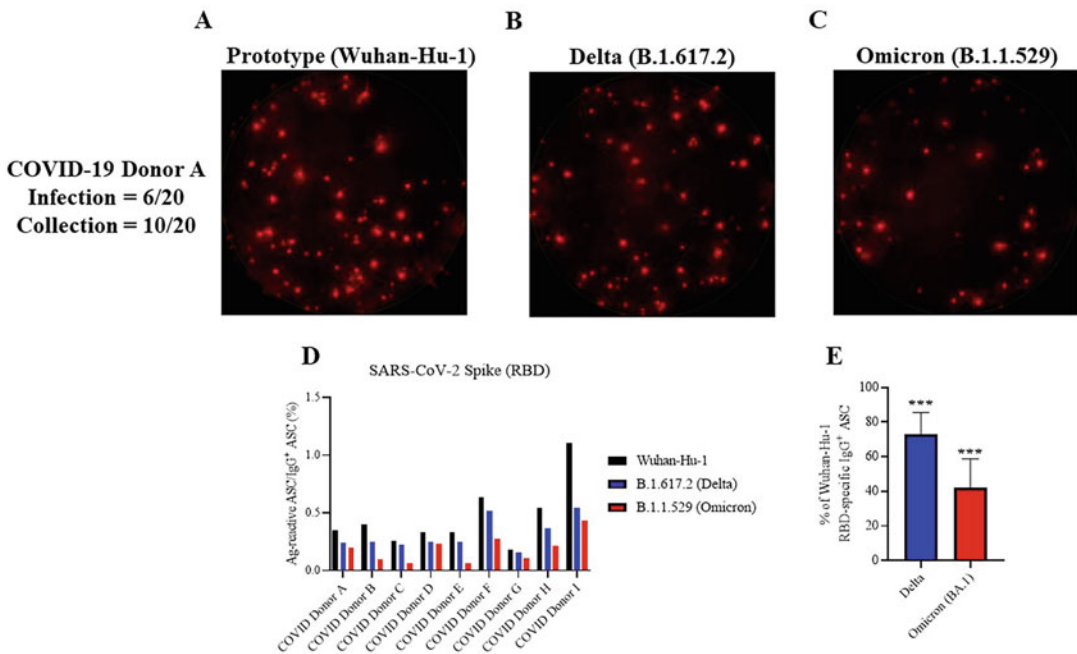


**Fig. 5** Inverted ImmunoSpot<sup>®</sup> enables assessment of B<sub>mem</sub> cross-reactivity against the receptor binding domain (RBD) of the homotypic prototype strain of SARS-CoV-2, and heterotypic antigenic variants of concern that emerged later in the COVID-19 pandemic. PBMC from nine convalescent COVID-19 donors with PCR-verified infection during the initial wave of SARS-CoV-2 infections caused by the prototype Wuhan-Hu-1 strain (collected prior to November 1, 2021, i.e., before the onset of the Delta and Omicron waves), were cryopreserved. After thawing, the PBMC were stimulated for 5 days *in vitro* to transition resting B<sub>mem</sub> into antibody-secreting cells (ASC). These *in vitro* stimulated PBMC were then seeded into an inverted ImmunoSpot<sup>®</sup> assay, leveraging IgG capture, to detect IgG<sup>+</sup> secretory footprints that captured RBD protein representative of the homotypic Wuhan-Hu-1, or heterotypic B.1.617.2 (Delta) or B.1.1.529 (Omicron) strains of SARS-CoV-2. Each of these RBD-variant specific secretory footprints was detected in single-color assays, first by the addition of the respective soluble His-tagged RBD antigen probe, followed by the addition of biotinylated anti-His mAb, and finally by the addition of SA-CTL-Red<sup>™</sup>. The individual secretory footprints, or spot-forming units (SFU), with reactivity against the His-tagged RBD probes were subsequently enumerated using ImmunoSpot<sup>®</sup> software. Representative well images for donor A are shown in panels **a–c** for the three RBD probes, as specified. **(d)** The percentage of IgG<sup>+</sup> ASC, following *in vitro* differentiation, exhibiting reactivity with the homotypic Wuhan-Hu-1, or heterotypic Delta or Omicron RBD probes. **(e)** The percentage of IgG<sup>+</sup> ASC reactive with the heterotypic Delta or Omicron RBD probes relative to the homotypic Wuhan-Hu-1 strain (denoted as 100%). Data are plotted as mean ± SD. Statistical significance was determined using an analysis of variance (ANOVA) and Bonferroni’s multiple comparisons post-hoc test. \*\*\**p* < 0.001

before, the PBMC are plated at the Goldilocks input number into replicate wells of an inverted B cell ImmunoSpot<sup>®</sup> assay. The “tag 1” labeled homotypic antigen probe (e.g., His tag) and the “tag 2” labeled heterotypic antigen probe (e.g., FLAG tag) are added simultaneously, at equimolar concentrations, followed by dual-color detection of SFU that bound an antigen probe. The ratio of “tag 1” single-color positive SFU and of “tag 1 + tag 2” double-color positive SFU is established, revealing the frequency of cross-

reactive ASC under equimolar conditions. Raising and lowering the concentration of the heterotypic antigen probe provides insights into the affinity of the individual homotype-primed  $B_{\text{mem}}$  for the heterotypic antigen.

### 1.12 Concluding Remarks

The aim of this chapter was to draw attention to the tremendous, thus far largely unrealized, potential of B cell ImmunoSpot<sup>®</sup> assays, and their potential to revolutionize immune diagnostics. Although the ELISPOT assay was originally introduced 40 years ago for detecting antigen-specific ASC [25, 26], it was T cell ELISPOT assays (introduced 5 years later [27]) that took the limelight. For the latter to occur, however, we needed to introduce fundamental modifications to the originally described protocol so that the assay lived up to its potential and was capable of reliably revealing secretory footprints of individual T cells responding to antigen ([28] and *see Note 27*). Our introduction of automated, objective, and scientifically validated software-assisted machine reading of T cell-derived secretory footprints [29] also largely contributed to the success of T cell ImmunoSpot<sup>®</sup> assays (*see Note 28*).

Despite being introduced earlier into the literature, B cell ImmunoSpot<sup>®</sup> assays have, thus far, not become a mainstay in B cell immune monitoring efforts. One likely reason is that for most antigens the classic protocol of directly absorbing the antigen to the assay membrane simply does not work (*see above*); only our recent introduction of the affinity coating approach [11] enables one to rapidly develop ImmunoSpot<sup>®</sup> assays for detecting ASC with specificity for essentially any affinity-tagged antigen of interest. But perhaps the primary reason why B cell ImmunoSpot<sup>®</sup> assays have not been sufficiently pursued until now is the widely held, and flawed, assumption that serum antibody measurements yield sufficient insight on underlying B cell-mediated adaptive humoral immunity. As outlined above, from the basic science perspective, this standpoint is no longer tenable. Importantly, a major component of the critical information pertaining to  $B_{\text{mem}}$ -mediated immunity is now easily attainable through the implementation of B cell ImmunoSpot<sup>®</sup> assays, as outlined above, and is neglected by studying antigen-specific serum reactivity/titers alone.

Ease of implementation, low cost, and moderate labor investment are major requirements for the success of any assay. The efficiency of B cell ImmunoSpot<sup>®</sup> in PBMC utilization has been repeatedly highlighted in this chapter (*see also see Note 23*) and is critical in clinical trial settings. Cryopreserved PBMC can be used without impairing B cell function [30], permitting batch testing of dozens of samples by a single investigator in a single experiment (and hundreds of samples with a well-trained team). Fully automated image analysis of the assay results is now available, along with retention of audit trails [10]. The reproducibility of B cell ImmunoSpot<sup>®</sup> is quite remarkable for a cellular assay [6], and the serial



dilution strategy detailed above permits to extend the upper and lower detection limits of the assay over orders of magnitude [6]. Moreover, B cell ImmunoSpot<sup>®</sup> assays have been shown to be suitable for regulated testing [31]. For all of the above reasons, we believe B cell ImmunoSpot<sup>®</sup> testing will soon become an indispensable component of the immune monitoring repertoire.

Detailed methodology for the affinity capture-based B cell ImmunoSpot<sup>®</sup> assay is described in another Chap. 15 contributed by Yao et al. in this volume [23]. This is the method of choice for establishing frequencies of antigen-specific ASC via the serial dilution strategy; including for all Ig classes, or IgG subclasses, simultaneously. Detailed methodology for the single-color, antigen-specific inverted B cell ImmunoSpot<sup>®</sup> assay described in Fig. 5 is detailed below. Both the direct and inverted ImmunoSpot<sup>®</sup> assay formats are also well-suited for assessment of ASC cross-reactivity. However, while direct ImmunoSpot<sup>®</sup> assays provide insights into the affinity distributions through studying spot morphologies, the inverted assay described in detail by Becza et al. [12] is the method of choice for such high-content analysis of antigen-specific ASC repertoires. Software solutions for B cell ImmunoSpot<sup>®</sup> analysis are detailed in another Chap. 5 of this volume by Karulin et al. [10].

---

## 2 Materials

### 2.1 Thawing of Cryopreserved PBMC

1. Class II biosafety cabinet (BSC).
2. Cryopreserved PBMC sample(s) (*see Note 23*).
3. 70% (v/v) ethanol (EtOH)
4. Conical tubes.
5. Sterile transfer pipette.
6. DNase-containing washing medium (prewarmed to 37 °C) (*see Note 29*).
7. Centrifuge capable of spinning 50 mL conical tubes at 330 × *g* (temperature set to 25 °C).
8. Complete B cell medium (BCM) (prewarmed to 37 °C) (*see Note 30*).
9. Ca<sup>2+</sup>, Mg<sup>2+</sup>-free phosphate-buffered saline (PBS), pH 7.2 (room temperature).
10. Parafilm.
11. CTL-LDC™ live/dead cell counting kit.
12. ImmunoSpot<sup>®</sup> S6 Ultimate 4 LED Analyzer, or suitable instrument equipped with the appropriate detection channels, running CTL's live/dead cell counting suite software.

### **2.2 *In Vitro* Polyclonal Stimulation of B Cells in PBMC**

1. B-Poly-S.
2. Volume-dependent, 48- or 24-well plate, or sterile culture flask (*see Note 31*).
3. Humidified incubator set at 37 °C, 5% CO<sub>2</sub>.

### **2.3 Four-Color, Antigen-Specific FluoroSpot Assay (Affinity Capture Coating)**

1. Commercially available, four-color Human Ig class (IgA, IgE, IgG, and IgM) affinity capture (His) FluoroSpot kit (*see Note 32*).
2. Commercially available, four-color Human IgG subclass affinity capture (His) FluoroSpot kit (*see Note 32*).
3. His-tagged recombinant protein (*see Notes 33 and 34*).
4. 190 proof (95% v/v) EtOH
5. Cell culture-grade water.
6. 96-well, round bottom dilution plate.
7. 0.05% Tween-PBS wash solution
8. 0.1 µm low-protein binding syringe filter
9. Plate washer.
10. Vacuum manifold.
11. ImmunoSpot<sup>®</sup> S6 Ultimate 4 LED Analyzer, or suitable instrument equipped with the appropriate detection channels, running CTL's ImmunoSpot<sup>®</sup> UV.

### **2.4 Single-Color, Antigen-Specific Inverted ImmunoSpot<sup>®</sup> Assay**

1. Commercially available, single-color inverted (His) human B cell ImmunoSpot<sup>®</sup> kit (*see Note 35*).
2. His-tagged recombinant protein (*see Note 36*).

---

## **3 Methods**

### **3.1 Thawing of Cryopreserved PBMC (Sterile Conditions)**

1. Place cryovial(s) into a 37 °C bead bath (or water bath, we prefer the former for sterility reasons) for 8 min to thaw.
2. Remove cryovial(s) and wipe with 70% EtOH inside the bio-safety cabinet (BSC) before unscrewing the cap(s).
3. Using a sterile pipette, transfer contents of cryovial(s) into a labeled conical tube.
4. Rinse each of the cryovials with 1 mL of prewarmed anti-aggregate solution. Transfer the rinse solution(s) to the conical tube(s) dropwise while swirling the tube to ensure adequate mixing of the cells and thawing medium.
5. Double the volume of the cell suspension by dropwise addition of warm anti-aggregate solution while swirling the tube to ensure adequate mixing of the cells and thawing medium.

6. Continue doubling the volume of the cell suspension by drop-wise addition of warm anti-aggregate solution while swirling the tube until the cryopreserved cell material has been diluted tenfold. If multiple cryovials are pooled, calculate using 1 mL of cryopreserved cell suspension + 9 mL of anti-aggregate solution to determine the necessary final resuspension volume.
7. Centrifuge balanced tubes at  $330 \times g$  for 10 min with the centrifuge brake on, at room temperature (RT).
8. Decant supernatant and resuspend the cell pellet(s) using prewarmed B cell medium (BCM) to achieve a cell density of approximately  $2\text{--}5 \times 10^6$  cells/mL. The number of PBMC recovered can be estimated at this point being 80% of the number frozen.
9. Pipet 15  $\mu$ L of live/dead cell counting dye onto a piece of parafilm to form a droplet.
10. Remove 15  $\mu$ L of cell suspension and combine with droplet of live/dead cell counting dye. Pipet up and down 3–5 times to mix the sample while avoiding the formation of bubbles.
11. Transfer 15  $\mu$ L of the cell and dye suspension into each chamber of a hemacytometer.
12. Determine live cell count and viability using CTL's live/dead cell counting suite.
13. Increase volume of cell suspension(s) with additional sterile PBS and centrifuge balanced tubes at  $330 \times g$  for 10 min with centrifuge brake on, unrefrigerated.
14. Decant supernatant and gently resuspend the cell pellet (s) using prewarmed BCM at a cell density to  $2 \times 10^6$  cells/mL.

### **3.2 In Vitro Polyclonal Stimulation of B Cells in PBMC (Sterile Conditions)**

1. Dilute CTL's B-Poly-S polyclonal stimulation reagent 1:500 into prewarmed BCM to achieve a final concentration of 2X. Into labeled sterile culture vessel, add the same volume of PBMC at  $2\text{--}4 \times 10^6$  cells/mL (*see Note 31*).
2. Transfer culture vessels (flasks or plates) into humidified incubator set at 37 °C, 5% CO<sub>2</sub> for 4–6 days (96–144 h).

### **3.3 Four-Color, Antigen-Specific FluoroSpot Assay (Affinity Capture Coating)**

1. Two days before plating cells (Day 2), prepare 70% EtOH and anti-His affinity capture antibody solutions.
2. Remove underdrain and pipet 15  $\mu$ L of 70% EtOH solution into the center of each well (or designated wells) of the assay plate. Immediately after the addition of the 70% EtOH solution to the entire plate (or designated wells), add 180  $\mu$ L/well of PBS. Decant and wash wells again with 180  $\mu$ L/well of PBS.
3. Decant the assay plate, replace underdrain, and immediately add 80  $\mu$ L/well of the anti-His affinity capture antibody

solution into each well (or designated wells, *see Note 37*) of the low autofluorescence PVDF-membrane plate provided with the kit.

4. Incubate the plate overnight at 4 °C in a humidified chamber.
5. The following day (Day 1), dilute the His-tagged protein(s) into Diluent A (provided with the kit) to the previously determined optimal concentration.
6. Decant the assay plate and wash wells with 180 µL/well of warm PBS. Immediately, add 80 µL/well of the corresponding His-tagged protein coating solution(s) into the designated wells.
7. Incubate the plate overnight at 4 °C in a humidified chamber.
8. On the day of the assay (Day 0), decant the assay plate and wash wells with 180 µL/well of warm PBS. Next, decant the plate and add 150 µL/well of prewarmed BCM to block the plate ( $\geq 1$  h at RT).
9. If using PBMC following *in vitro* polyclonal stimulation, collect the cell suspension(s) and transfer into labeled conical tube(s). Keep the cells warm during processing. Wash culture vessel's interior with sterile warm PBS to collect residual PBMC and transfer into the corresponding conical tube(s). Increase volume to fill the tube with additional warm PBS and then centrifuge balanced tubes at  $330 \times g$  for 10 min nonrefrigerated, centrifuge with brake on. Alternatively, follow the procedures detailed above to obtain freshly isolated PBMC, or to thaw PBMC that were previously cryopreserved, if prior *in vitro* stimulation is not required to elicit antigen-specific ASC activity in the sample(s).
10. Decant supernatant and resuspend the cell pellet(s) using prewarmed BCM to achieve a cell density of  $\sim 2\text{--}5 \times 10^6$  cells/mL (the cell number recovered at this point can be estimated to be 50% of the number of cells frozen).
11. Pipet 15 µL of live/dead cell counting dye onto a piece of parafilm to form a droplet.
12. Remove 15 µL of cell suspension and combine with droplet of live/dead cell counting dye. Pipet up and down 3–5 times to mix the sample while avoiding the formation of bubbles.
13. Transfer 15 µL of the cell and dye suspension into each chamber of a hemacytometer.
14. Determine live cell count and viability using CTL's live/dead cell counting suite.
15. Increase volume of cell suspension(s) with additional sterile warm PBS and centrifuge balanced tubes at  $330 \times g$  for 10 min with centrifuge brake on, unrefrigerated.

16. Decant supernatant and resuspend the cell pellet(s) using prewarmed BCM at  $2 \times 10^6$  PBMC/mL.
17. Decant the BCM used for blocking the assay plate and replace with 100  $\mu$ L/well of prewarmed BCM.
18. If applicable, e.g., for Goldilocks number determinations or accurate frequency measurements, prepare PBMC serial dilution series in a round-bottom 96-well polystyrene plate to match the plate layout shown in Fig. 5a of the chapter by Yao et al. in this volume [23] before transferring the PBMC into the ImmunoSpot<sup>®</sup> assay.
19. Incubate cells in the assay plate for 16–18 h at 37 °C, 5% CO<sub>2</sub>.
20. After completion of the assay incubation period, decant (or reutilize) cells and wash plate two times with warm PBS (200  $\mu$ L/well), followed by two additional washing steps with 0.05% Tween-PBS wash solution (*see Note 38*).
21. Prepare anti-Ig class/subclass-specific detection antibody solution(s) according to kit protocol and pass through 0.1  $\mu$ m low-protein binding syringe filter to remove any protein aggregates.
22. Decant 0.05% Tween-PBS wash solution, add 80  $\mu$ L/well of the anti-Ig class/subclass-specific detection antibody solution into designated wells, and incubate for 2 h at RT (protected from light).
23. Wash plate(s) two times with 0.05% Tween-PBS wash solution.
24. Prepare tertiary solution by following kit protocol and pass through 0.1  $\mu$ m low-protein binding syringe filter to remove any aggregates.
25. Decant 0.05% Tween-PBS wash solution, add 80  $\mu$ L/well of tertiary solution into designated wells, and incubate for 1 h at RT (protected from light).
26. Wash plates(s) twice with distilled water.
27. Remove protective underdrain and place plate face down on vacuum manifold. Completely fill the backside of the plate with distilled water and apply vacuum to draw water through the membrane (“back to front”) (*see Note 39*).
28. Allow plate to dry completely, protected from light (*see Note 40*).
29. Scan and count plate(s) with suitable analyzer equipped with the appropriate detection channels (*see Note 18*).

**3.4 Single-Color,  
Antigen-Specific  
Human IgG-Inverted  
ImmunoSpot<sup>®</sup> Assay**

1. One day before plating cells (Day 1), prepare 70% EtOH and anti-human IgG capture antibody solutions.
2. Remove underdrain and pipet 15  $\mu$ L of 70% EtOH solution into the center of each well (or designated wells) of the assay

plate. Immediately after addition of the 70% EtOH solution to the entire plate (or designated wells), add 180  $\mu\text{L}$ /well of PBS. Decant and wash wells again with 180  $\mu\text{L}$ /well of PBS.

3. Decant the assay plate, replace underdrain, and immediately add 80  $\mu\text{L}$ /well of the anti-human IgG capture antibody solution into each well (or designated wells) of the low autofluorescence PVDF-membrane plate provided with the kit.
4. Incubate the plate overnight at 4 °C in a humidified chamber.
5. On the day of the assay (Day 0), decant the assay plate and wash wells with 180  $\mu\text{L}$ /well of PBS. Next, decant the plate and add 150  $\mu\text{L}$ /well of prewarmed BCM to block the plate ( $\geq 1$  h at RT).
6. If using PBMC following polyclonal stimulation, collect the cell suspension(s) and transfer into labeled conical tube(s). Rinse interior of the culture vessel to recover all cells and transfer into the corresponding conical tube(s). Increase volume to fill up tube with additional PBS and then centrifuge balanced tubes at  $330\times g$  for 10 min with centrifuge brake on, at RT. Alternatively, thaw previously cryopreserved PBMC as detailed above if prior in vitro stimulation is not required to elicit antigen-specific ASC activity in the sample(s).
7. Decant supernatant and resuspend the cell pellet(s) using prewarmed BCM to achieve a cell density of approximately  $2\text{--}5 \times 10^6$  cells/mL (this number can be estimated to be 50% of that prior to the stimulation culture).
8. Pipet 15  $\mu\text{L}$  of live/dead cell counting dye onto a piece of parafilm to form a droplet.
9. Remove 15  $\mu\text{L}$  of cell suspension and combine with droplet of live/dead cell counting dye. Pipet up and down 3–5 times to mix the sample while avoiding the formation of bubbles.
10. Transfer 15  $\mu\text{L}$  of the cell and dye suspension into each chamber of a hemacytometer.
11. Determine live cell count and viability using CTL's live/dead cell counting suite.
12. Increase volume of cell suspension(s) with additional sterile warm PBS and centrifuge balanced tubes at  $330\times g$  for 10 min with centrifuge brake on, at RT.
13. Decant supernatant and resuspend the cell pellet(s) using prewarmed BCM at approximately  $1 \times 10^6$  PBMC/mL.
14. Decant the BCM used for blocking the assay plate and replace with 100  $\mu\text{L}$ /well of prewarmed BCM to block the plate.
15. If the Goldilocks number has already been established for the PBMC(s), plate cells at that number into the ImmunoSpot<sup>®</sup>

assay. If that number is unknown, prepare serial dilution of PBMC (or other single-cell suspension) accordingly, and then transfer into the ImmunoSpot<sup>®</sup> assay plate.

16. Incubate cells in the assay plate for 16–18 h at 37 °C, 5% CO<sub>2</sub>.
17. After completion of the assay incubation period, remove plate and decant cells. Wash plate two times with PBS (200 µL/well), followed by two additional washing steps with 0.05% Tween-PBS wash solution (*see Note 38*).
18. Prepare His-tagged antigen probe solution at optimized concentration and pass through 0.1 µm low-protein binding syringe filter to remove any protein aggregates.
19. Decant 0.05% Tween-PBS wash solution, add 80 µL/well of His-tagged antigen probe solution into designated wells, and incubate for 2 h at RT (protected from light).
20. Wash plate(s) two times with 0.05% Tween-PBS wash solution.
21. Prepare anti-His detection antibody solution according to kit protocol and pass through 0.1 µm low-protein binding syringe filter to remove any aggregates.
22. Decant 0.05% Tween-PBS wash solution, add 80 µL/well of anti-His detection antibody solution into designated wells, and incubate for 1 h at RT (protected from light).
23. Wash plate(s) two times with 0.05% Tween-PBS wash solution.
24. Prepare tertiary solution according to kit protocol and pass through 0.1 µm low protein binding syringe filter to remove any aggregates.
25. Wash plates(s) twice with distilled water.
26. Remove protective underdrain and place plate face down on vacuum manifold. Completely fill the backside of the plate with distilled water and apply vacuum to draw water through the membrane (“back to front”) (*see Note 39*).
27. Allow plate to dry completely, protected from light (*see Note 40*).
28. Scan and count plate(s) with suitable analyzer equipped with the appropriate detection channel (*see Note 18*).

---

## 4 Notes

1. As enzyme-linked immunospot (ELISPOT) and FluoroSpot assays differ only in the modality of detecting secretory footprints of cells on membranes, we collectively refer to both as ImmunoSpot<sup>®</sup> assays. In the former, the detection antibody is tagged to enable the engagement of an enzymatic reaction that results in the local precipitation of a substrate visible under

white light. In the latter, the plate-bound detection antibodies are visualized via fluorescent tags using appropriate excitation and emission wavelengths. Data provided in the chapter in this volume by Yao et al. [23] establish that ELISPOT and Fluoro-Spot assays have equal sensitivity for detecting antibody-secreting cell (ASC)-derived secretory footprints.

2. In proliferating germinal center B cells (GCB), somatic hypermutation (SHM) introduces random mutations into the variable regions of the B cell receptors (BCR) responsible for antibody binding. As a result, subclones endowed with improved, or decreased, BCR binding affinity for the antigen are generated. GCB subclones that possess an increased BCR affinity for antigen are positively selected to proliferate and undergo further rounds of SHM to further improve BCR affinity. Collectively, the positive selection of GCB subclones with improved binding for antigen underlies the progressive affinity maturation of the ensuing antibody response.
3. B cell antigen receptors (BCR) are the membrane-anchored forms of secreted immunoglobulin (Ig) molecules (commonly referred to as antibodies). Surface BCR are encoded by the same Ig class/subclass and possess an identical antigen specificity to the antibody that a B cell will secrete once it differentiates into an ASC, such as a plasma cell (PC).
4. As the concentration of antigen declines with time, only those germinal center B (GCB) cells with the highest affinity will continue to successfully compete for antigen binding, and only the latter will continue to proliferate and undergo progressive SHM to eventually differentiate along the PC lineage.
5. The half-life of different Ig classes, and IgG subclasses, in serum is variable and relatively short *in vivo*. The half-life of IgG1, IgG2, and IgG4 in humans is 21–28 days, whereas for IgG3 it is ~1 week [32]. For IgA and IgM, their half-lives are even shorter (3–7 days) [33, 34] and IgE has the shortest half-life in serum, ~2–3 days [35].
6. The extended half-life of serum IgG *in vivo* is dependent on its interactions with FcRn [36, 37] which protects it from catabolism and enables IgG recycling. Likewise, the *in vivo* half-life of other antibody classes such as IgA, IgE, and IgM are also greatly extended when in association with Ig-binding surface receptors [35, 38].
7. IgE secreted by B cells can bind to high-affinity Fc receptors (FcεRI) expressed on mast cells and basophils and endow these cells with antigen-recognition properties. IgA antibodies are secreted to mucosal surfaces.
8. Traditional B cell ELISPOT assays have been performed by direct coating of the assay membrane with the antigen of



interest. However, many (in fact, most) antigens do not adsorb sufficiently to the membrane to enable reliable detection of ASC-derived secretory footprints. We have overcome this limitation by introducing an affinity coating approach for achieving high-density antigen absorption to the assay membrane [11].

9. These samples were collected early in the COVID-19 pandemic when the prototype Wuhan-Hu-1 strain of the SARS-CoV-2 virus was circulating, and the testing was done with Spike and Nucleocapsid (NCAP) antigens that corresponded to the original Wuhan-Hu-1 strain. Thus, homotypic B cell memory was studied.
10. While ImmunoSpot<sup>®</sup> enables measurement of a single ASC within a bulk population of cells, flow cytometry falls short of detecting antigen-specific cells when they are present as very low-frequency events. In ImmunoSpot<sup>®</sup> assays, there is no inherent lower limit of detection. If, e.g., 3 million PBMC are plated at  $3 \times 10^5$  PBMC across 10 replicate wells, 1 in 3 million is the detection limit, etc. Importantly, owing to increased Poisson noise occurring with such low-frequency measurements, the number of replicate wells evaluated needs to be increased accordingly to obtain accurate low-frequency measurements. As shown in Fig. 3, antigen-specific B<sub>mem</sub> quite frequently occur in low frequencies.
11. To establish the frequency of antigen-specific ASC among all ASC-producing IgM/IgG/IgA/IgE or all four IgG subclasses (IgG1-IgG4) requires ~2 million PBMC (that can be isolated from 2 to 3 mL of blood) when done according to our protocols (*see* also **Note 23**). To obtain the same information by flow cytometry, up to ten-fold more cells would be required [39, 40].
12. For details of four-color B cell ImmunoSpot<sup>®</sup> detection, see the chapter by Yao et al. in this volume [23]. Flow cytometry does not reliably reveal the class/subclass of Ig produced by the individual B cell because surface BCR expression can be highly variable and this is an underappreciated complexity of probe staining. In particular, in the case of IgG<sup>+</sup> ASC, they express little if any surface BCR and this undermines assessment of their antigen specificity and subclass usage using traditional surface staining approaches. Consequently, fixation and intracellular staining are required to define the IgG subclass usage of these cells (a procedure that results in substantial cell loss in the sample).
13. Each investigator in our laboratory can routinely test, in a single experiment, 10–20 PBMC samples for reactivity against a panel of antigens, assessing the frequency of ASC producing

each of the Ig classes and IgG subclasses (see also the chapter by Yao et al. in this volume [23]). With additional logistical refinements, this throughput is readily scalable upward.

14. For most antigens we have investigated thus far (SARS-CoV-2 NCAP and receptor binding domain (RBD) proteins, the HCMV gH pentamer complex, EBV EBNA1, and OVA), we have been unsuccessful in establishing reliable B cell ImmunoSpot<sup>®</sup> assays when following the classic protocol in which the antigen is directly absorbed to the membrane irrespective of how high an antigen concentration was used for coating. In contrast, our recent introduction of the affinity coating strategy [11] generated pristine results with each of these antigens. We succeeded with direct coating only with recombinant hemagglutinin proteins of seasonal influenza viruses or the full-length trimeric Spike protein of SARS-CoV-2, albeit having to use very high antigen coating concentrations (exceeding 20 µg/mL) to achieve high-quality secretory footprint formation.
15. In addition to detecting antigen-specific, B cell-derived secretory footprints on affinity-coated plates, as described here, it is also possible to detect such cells via the inverted ImmunoSpot<sup>®</sup> approach. In the latter, the Ig secretory footprint is captured irrespective of the ASC's specificity (e.g., by coating the membrane with an anti-IgG capture antibody) and the antigen-specific B cells' secretory footprints among all those retained on the membrane are detected by the capture of labeled antigen. Such inverted assays work perfectly when the frequency of antigen-specific B cell footprints is high among all secretory footprints captured, but are challenging for the detection of low-frequency events. Inverted assays are described in detail in the chapter by Becza et al. in this volume [12]. While direct assays permit the capture of all Ig classes or subclasses produced by antigen-specific ASC via four-color ImmunoSpot<sup>®</sup> detection (see the chapter by Yao et al. in this volume [23]), the inverted assay detects only the selected Ig class, e.g., IgG<sup>+</sup> ASC.
16. B cell ImmunoSpot<sup>®</sup> data can be expressed as spot-forming units (SFU) per cell input per well to determine the frequency of antigen-specific cells. However, owing to considerable inter-individual variations in the abundance of total Ig class/subclass producing ASC in test samples following polyclonal stimulation, and the prevalence of IgG [6], it is better to report data as the frequency of ASC producing a given Ig class/subclass among all ASC producing that Ig class/subclass.
17. ASC secrete Ig in an undirected fashion into 3D space. The antibody released toward the membrane will be captured as a secretory footprint; however, the remainder of the secreted

antibody will diffuse away from the cell and is diluted into the culture supernatant. As the concentration of diffused antibodies increases in the culture medium, these antibodies are captured on the membrane distantly from the source ASC, increasing the background signal in the assay and undermining the resolution of individual secretory footprints. Such an elevated background in an ImmunoSpot<sup>®</sup> assay is termed an ELISA effect that can obscure the accurate counting, or even detection of secretory footprints [6].

18. The chapter by Karulin et al. in this volume [10] introduces machine learning-based spot-forming unit (SFU) analysis that can partially compensate for ELISA effects and SFU crowding, thus extending the linear range of accurate quantification for cell numbers plated per well and SFU detected.
19. When performing such serial dilution experiments, using 4 replicate wells per cell input plated, and linear regression of the SFU frequency through extrapolation from the mean of these 4 replicates, that calculated frequency was very close to the frequencies established by relying on just one replicate well per cell input dilution (see the chapter by Yao et al. in this volume [23], and N. Becza, manuscript in preparation). Thus, serial dilutions involving single wells for each cell dilution, progressing in a 1 + 1 (two-fold) dilution series is a valid option for establishing accurate SFU frequencies and greatly reduces the cell numbers and reagents required.
20. We failed to detect SARS-CoV-2 Spike or NCAP antigen-specific, class-switched (IgG or IgA) ASC in individuals collected prior to the COVID-19 pandemic that by definition would be immunologically naive to the SARS-CoV-2 virus [6]. However, IgM<sup>+</sup> ASC reactivity against these antigens in the pre-COVID-19 donor cohort population was ambiguous because the current polyclonal stimulation approach also results in the differentiation of naive IgM<sup>+</sup> B cells, which may express broadly reactive specificities and can generate secretory footprints in negative control wells. In contrast, all subjects with PCR-verified infection, harbored S and N antigen-specific IgG<sup>+</sup> ASC. These findings are consistent with the notion that clonal expansions to detectable frequency levels, class-switching, and affinity maturation (all features of B<sub>mem</sub>) are needed for detecting antigen-specific B cells in ImmunoSpot<sup>®</sup> assays. Therefore, it appears that detection of class-switched, antigen-specific ASC in ImmunoSpot<sup>®</sup> assays implies prior *in vivo* priming of B<sub>mem</sub> with (cognate or cross-reactive) specificity for the test antigen.

21. Thus far, we have not seen evidence for class-switching of  $B_{\text{mem}}$  during short-term in vitro polyclonal stimulation using R848 plus IL-2.
22. So far, having studied “healthy volunteers” exclusively, we only detect  $\text{IgE}^+$  ASC following in vitro stimulation with agonistic anti-CD40 mAb plus IL-4 and IL-21, but not after stimulation with R848 plus IL-2 [41]. Thus, our detection system enables identification of  $\text{IgE}^+$  ASC, but whether  $\text{IgE}^+$   $B_{\text{mem}}$  exist in vivo, or whether they switch de novo to  $\text{IgE}$  in vivo or in vitro is controversial [42, 43].
23. If special protocols are followed, PBMC can be frozen without impairing the B cells’ functionality ([30] and N. Becza manuscript in preparation). Thus, by freezing B cells of a sample in several aliquots, the same PBMC can be tested repeatedly, reproducing the results of the previous experiment with high accuracy [6], or for extending those studies, e.g., for assessing the affinity distribution of the antigen-specific  $B_{\text{mem}}$  repertoire. Of note, when planning the numbers of PBMC to be frozen per cryovial, as a rule of thumb, one can anticipate recovery of ~50% of PBMC initially frozen after these cells are thawed and have undergone 5 days of in vitro polyclonal stimulation to promote terminal differentiation of resting  $B_{\text{mem}}$  into ASC. It is also important to note that any number of PBMC between 1 and 10 million can be frozen per cryovial permitting the optimization of PBMC utilization when planning experiments (N. Becza, manuscript in preparation).
24. While the potential of B cell ImmunoSpot<sup>®</sup> assays to establish affinity distributions is embedded in the nature of the assay, this potential has not been realized yet. The chapter by Becza et al. in this volume [12] is the first step in this direction. To progress along these lines is one of the major focuses in our laboratory.
25. It can be assumed that after vaccination with the prototype Wuhan-Hu-1 strain Spike antigen, in addition to T-cell immunity directed against shared antigenic determinants of Spike variants, heterotype-specific, cross-reactive B cell memory for the receptor binding domain (RBD) mediates the partial protection seen toward newly emerging antigenic variants of this virus. Such SARS-CoV-2 variants evade the first wall (reflected by serum antibodies) and are thus capable of causing infections, but the engagement of cross-reactive  $B_{\text{mem}}$  (the second wall) can still convey protection from severe disease through rapidly generating a quasi-secondary neutralizing antibody response against the mutated RBD of the new variant.
26. In our ongoing studies, we find that ~40% Wuhan-Hu-1 infection-elicited  $B_{\text{mem}}$  are cross-reactive with the Omicron (BA.1) variant (Fig. 5 and Liu et al., work in progress).

27. Our introduction of the PVDF membrane to T-cell ELISPOT assays [28], with its by far superior capture antibody adsorption properties [44], has been key for improving our ability to detect secretory footprints to the point needed for transforming ImmunoSpot<sup>®</sup> into the robust T-cell monitoring platform it has become for detecting rare – even very rare – antigen-specific T cells *ex vivo*, in freshly isolated PBMC or other lymphoid cell material. We refer to Figure 1 in [45] to appreciate the difference in assay performance using the PVDF membrane vs. the previously used mixed cellulose ester membrane.
28. The shape of secretory footprints (spot morphologies) produced by T cells follows simple rules since the capture antibody's (i.e., an anti-cytokine-specific mAb) affinity for the analyte to be detected is high and fixed. Consequently, only the quantity of analyte (cytokine) produced by the T cell will define the morphology of the resulting secretory footprint [16]. Predictable (log normal, [46]) spot sizes permit objective automated size gating [47]. However, ASC-derived secretory footprints in antigen-coated wells are primarily defined by the affinity of the secreted antibody for the membrane-bound antigen. Thus, the formation of ASC-derived secretory footprints follows a different set of rules, and hence requires a fundamentally different analytical approach. The chapter contributed by Karulin et al. in this volume [10] introduces a software solution suited for accurate, high-throughput, and high-content B cell ImmunoSpot<sup>®</sup> analysis.
29. Thawing of cryopreserved cells causes a fraction of the cells (up to 30%) to die, and the DNA released from such cells can cause clumping of the thawed cell material. This cell clumping can be reduced, if not completely eliminated, by including an immunologically neutral endonuclease, Benzonase. Ready-to-use Benzonase-containing serum-free wash solutions are available: CTL anti-aggregate Wash<sup>™</sup> 20X solution.
30. A suitable assay medium for use in B cell ImmunoSpot<sup>®</sup> is RPMI 1640 with 10% FCS, 2 mM L-glutamine, 100 U/mL penicillin, 100 µg/mL streptomycin, 8 mM HEPES, and 50 µM 2-mercaptoethanol.
31. The volume of *in vitro* stimulation cultures can be scaled up or down accordingly, but we recommend keeping the cell density of PBMC at approximately  $1-2 \times 10^6$  cells/mL. Smaller *in vitro* stimulation cultures can be initiated in 48- or 24-well plates with a final volume of 1 or 2 mL, respectively. Be sure to fill empty wells in tissue culture plates with sterile PBS to avoid dehydration of cell cultures. For larger volumes, use appropriate tissue culture flasks, upright or laying, with the culture medium between 0.5 and 1 cm in height.

32. Kit is suited for detecting either antigen-specific ASC that differentiated *in vivo*, or antigen-specific B<sub>mem</sub> that have been polyclonally stimulated *in vitro* to promote their transition to ASC. Each kit contains anti-His capture antibody, Ig class-specific (IgA, IgE, IgG, and IgM) detection reagents, diluent buffers, low autofluorescence PVDF-membrane plates, and polyclonal B cell activator (B-Poly-S). Alternatively, IgG class-specific (IgG1, IgG2, IgG3, and IgG4) detection reagents can be substituted in the context of such four-color B cell ImmunoSpot<sup>®</sup> assays.
33. Traditional B cell ELISPOT assays have been performed by direct coating of the assay membrane with the antigen of interest. However, many (in fact, most) antigens do not adsorb sufficiently to the membrane to enable reliable detection of ASC-derived secretory footprints. We have overcome this limitation by introducing an affinity coating approach for achieving high-density antigen absorption to the assay membrane [11].
34. We recommend optimizing the concentration of His-tagged protein(s) used for affinity capture coating. A concentration of 10 µg/mL His-tagged protein has yielded well-formed secretory footprints for most antigens, but increased concentrations of the anti-His affinity capture antibody and/or His-tagged protein may be required to achieve optimal assay performance [11].
35. Kit is suited for detecting either antigen-specific ASC that differentiated *in vivo*, or antigen-specific B<sub>mem</sub> that have been polyclonally stimulated *in vitro* to promote their transition to ASC. Each kit contains pan anti-human IgG capture antibody, anti-His detection reagents, diluent buffers, low autofluorescence PVDF-membrane plates, and polyclonal B cell activator (B-Poly-S).
36. The optimal concentration of affinity (His)-tagged antigen probe used for detection of all antigen-specific secretory footprints (e.g., SFU), low- or high-affinity alike, should be determined empirically.
37. If the entire plate will not be coated with the anti-His affinity capture antibody solution, the remainder of the EtOH prewet wells should receive 80 µL/well of PBS.
38. Plate washes may also be performed manually. For automated washing, the pin height and flow rate should be customized to avoid damaging the assay membranes, which is the case for the CTL 405LSR plate washer.
39. Lowering nonspecific background staining, and reduction of “hot spots” in the center of the assay wells, is achieved through performing the “back to front” water filtration technique.

40. To completely dry plates, blot assay plate(s) on paper towels to remove residual water before either placing them in a running laminar flow hood at a 45° angle for >20 min or placing face down on paper towels for >2 h in a dark drawer/cabinet. Do not dry assay plates at temperatures exceeding 37 °C as this may cause the membrane to warp or crack. Fluorescent spots may not be readily visible while the membrane is still wet and the background fluorescence may be elevated. Scan and count plates only after membranes have dried completely.

---

## Acknowledgments

We wish to thank the R&D and the Software Development teams at CTL for their continued support and technological innovation that made our B cell ImmunoSpot<sup>®</sup> endeavor possible. We thank Drs. Alexey Y. Karulin and Graham Pawelec for in-depth discussions of the subject matter, and Diana Roen for carefully proofreading the manuscript, and also Gregory Kovacs for his support in the generation of graphic illustrations. All efforts were funded from CTL's research budget.

**Conflicts of Interest** P.V.L. is Founder, President, and CEO of CTL, a company that specializes in immune monitoring by ImmunoSpot<sup>®</sup>. Z.L., N.B., A.V.V., and G.A.K are employees of CTL. J.B. was a summer intern at CTL when he developed the tetanus toxoid heavy chain (TTHc)-specific B cell ImmunoSpot<sup>®</sup> assay and contributed the frequency measurements of TTHc-specific B<sub>mem</sub> cells incorporated in Fig. 3.

## References

1. Akkaya M, Kwak K, Pierce SK (2020) B cell memory: building two walls of protection against pathogens. *Nat Rev Immunol* 20(4): 229–238. <https://doi.org/10.1038/s41577-019-0244-2>
2. Inoue T, Shinnakasu R, Kurosaki T (2021) Generation of high quality memory B cells. *Front Immunol* 12:825813. <https://doi.org/10.3389/fimmu.2021.825813>
3. Palm AE, Henry C (2019) Remembrance of things past: long-term B cell memory after infection and vaccination. *Front Immunol* 10: 1787. <https://doi.org/10.3389/fimmu.2019.01787>
4. Lightman SM, Utley A, Lee KP (2019) Survival of long-lived plasma cells (LLPC): piecing together the puzzle. *Front Immunol* 10:965. <https://doi.org/10.3389/fimmu.2019.01787>
5. Robinson MJ, Ding Z, Dowling MR, Hill DL, Webster RH, McKenzie C, Pitt C, O'Donnell K, Mulder J, Brodie E, Hodgkin PD, Wong NC, Quast I, Tarlinton DM (2023) Intrinsically determined turnover underlies broad heterogeneity in plasma-cell lifespan. *Immunity* 56(7):1596–1612. e1594. <https://doi.org/10.1016/j.immuni.2023.04.015>
6. Wolf C, Koppert S, Becza N, Kuerten S, Kirchenbaum GA, Lehmann PV (2022) Antibody levels poorly reflect on the frequency of memory B cells generated following SARS-CoV-2, seasonal influenza, or EBV infection. *Cell* 11(22). <https://doi.org/10.3390/cells11223662>

7. Murata T, Sugimoto A, Inagaki T, Yanagi Y, Watanabe T, Sato Y, Kimura H (2021) Molecular basis of Epstein-Barr virus latency establishment and lytic reactivation. *Viruses* 13(12). <https://doi.org/10.3390/v13122344>
8. Terlutter F, Caspell R, Nowacki TM, Lehmann A, Li R, Zhang T, Przybyla A, Kuerten S, Lehmann PV (2018) Direct detection of T- and B-memory lymphocytes by ImmunoSpot(R) assays reveals HCMV exposure that serum antibodies fail to identify. *Cells* 7(5). <https://doi.org/10.3390/cells7050045>
9. Kuerten S, Pommerschein G, Barth SK, Hohmann C, Milles B, Sammer FW, Duffy CE, Wunsch M, Rovituso DM, Schroeter M, Addicks K, Kaiser CC, Lehmann PV (2014) Identification of a B cell-dependent subpopulation of multiple sclerosis by measurements of brain-reactive B cells in the blood. *Clin Immunol* 152(1–2):20–24. <https://doi.org/10.1016/j.clim.2014.02.014>
10. Karulin AY, Megyesi Z, Kirchenbaum GA, Lehmann PV (2023) Artificial intelligence-based counting algorithm enables accurate and detailed analysis of the broad-spectrum of spot morphologies observed in antigen-specific B cell ELISPOT and FLUOROSPOT assays. *Methods Mol Biol*
11. Koppert S, Wolf C, Becza N, Sautto GA, Franke F, Kuerten S, Ross TM, Lehmann PV, Kirchenbaum GA (2021) Affinity tag coating enables reliable detection of antigen-specific B cells in Immunospot assays. *Cell* 10(8). <https://doi.org/10.3390/cells10081843>
12. Becza N, Liu Z, Chepke J, Gao X, Kirchenbaum GA, Lehmann PV (2023) Assessing the affinity spectrum of the antigen-specific B cell repertoire via ImmunoSpot®. *Methods Mol Biol*
13. Ansotegui IJ, Melioli G, Canonica GW, Caraballo L, Villa E, Ebisawa M, Passalacqua G, Savi E, Ebo D, Gomez RM, Luengo Sanchez O, Oppenheimer JJ, Jensen-Jarolim E, Fischer DA, Haahtela T, Antila M, Bousquet JJ, Cardona V, Chiang WC, Demoly PM, DuBuske LM, Ferrer Puga M, Gerth van Wijk R, Gonzalez Diaz SN, Gonzalez-Estrada A, Jares E, Kalpaklioglu AF, Kase Tanno L, Kowalski ML, Ledford DK, Monge Ortega OP, Morais Almeida M, Pfaar O, Poulsen LK, Pawankar R, Renz HE, Romano AG, Rosario Filho NA, Rosenwasser L, Sanchez Borges MA, Scala E, Senna GE, Sisul JC, Tang MLK, Thong BY, Valenta R, Wood RA, Zuberbier T (2020) IgE allergy diagnostics and other relevant tests in allergy, a world allergy organization position paper. *World Allergy Organ J* 13(2):100080. <https://doi.org/10.1016/j.waojou.2019.100080>
14. Abreu RB, Kirchenbaum GA, Clutter EF, Sautto GA, Ross TM (2020) Preexisting subtype immunodominance shapes memory B cell recall response to influenza vaccination. *JCI Insight* 5(1). <https://doi.org/10.1172/jci.insight.132155>
15. Sanyal M, Holmes TH, Maecker HT, Albrecht RA, Dekker CL, He XS, Greenberg HB (2019) Diminished B-cell response after repeat influenza vaccination. *J Infect Dis* 219(10):1586–1595. <https://doi.org/10.1093/infdis/jiy685>
16. Karulin AY, Lehmann PV (2012) How ELISPOT morphology reflects on the productivity and kinetics of cells' secretory activity. *Methods Mol Biol* 792:125–143. [https://doi.org/10.1007/978-1-61779-325-7\\_11](https://doi.org/10.1007/978-1-61779-325-7_11)
17. Lu LL, Suscovich TJ, Fortune SM, Alter G (2018) Beyond binding: antibody effector functions in infectious diseases. *Nat Rev Immunol* 18(1):46–61. <https://doi.org/10.1038/nri.2017.106>
18. Stavnezer J, Guikema JE, Schrader CE (2008) Mechanism and regulation of class switch recombination. *Annu Rev Immunol* 26:261–292. <https://doi.org/10.1146/annurev.immunol.26.021607.090248>
19. Chu RS, Targoni OS, Krieg AM, Lehmann PV, Harding CV (1997) CpG oligodeoxynucleotides act as adjuvants that switch on T helper 1 (Th1) immunity. *J Exp Med* 186(10):1623–1631. <https://doi.org/10.1084/jem.186.10.1623>
20. Yip HC, Karulin AY, Tary-Lehmann M, Hesse MD, Radeke H, Heeger PS, Trezza RP, Heinzl FP, Forsthuber T, Lehmann PV (1999) Adjuvant-guided type-1 and type-2 immunity: infectious/noninfectious dichotomy defines the class of response. *J Immunol* 162(7):3942–3949
21. Webb NE, Bernshtein B, Alter G (2021) Tissues: the unexplored frontier of antibody mediated immunity. *Curr Opin Virol* 47:52–67. <https://doi.org/10.1016/j.coviro.2021.01.001>
22. Wang TT, Sewatanon J, Memoli MJ, Wrammert J, Bournazos S, Bhaumik SK, Pinsky BA, Chokephaibulkit K, Onlamoon N, Pattanapanyasat K, Taubenberger JK, Ahmed R, Ravetch JV (2017) IgG antibodies to dengue enhanced for FcγRIIIA binding determine disease severity. *Science* 355(6323):395–398. <https://doi.org/10.1126/science.aai8128>



23. Yao L, Becza N, Maul-Pavicic A, Chepke J, Kirchenbaum GA, Lehmann PV (2023) Four-color ImmunoSpot® assays requiring only 1–3 mL of blood permit precise frequency measurements of antigen-specific B cells secreting immunoglobulins of all four classes and subclasses. *Methods Mol Biol*
24. Matz HC, McIntire KM, Ellebedy AH (2023) Persistent germinal center responses: slow-growing trees bear the best fruits. *Curr Opin Immunol* 83:102332. <https://doi.org/10.1016/j.coi.2023.102332>
25. Czerkinsky CC, Nilsson LA, Nygren H, Ouchterlony O, Tarkowski A (1983) A solid-phase enzyme-linked immunospot (ELISPOT) assay for enumeration of specific antibody-secreting cells. *J Immunol Methods* 65(1–2): 109–121. [https://doi.org/10.1016/0022-1759\(83\)90308-3](https://doi.org/10.1016/0022-1759(83)90308-3)
26. Sedgwick JD, Holt PG (1983) A solid-phase immunoenzymatic technique for the enumeration of specific antibody-secreting cells. *J Immunol Methods* 57(1–3):301–309. [https://doi.org/10.1016/0022-1759\(83\)90091-1](https://doi.org/10.1016/0022-1759(83)90091-1)
27. Czerkinsky C, Andersson G, Ekre HP, Nilsson LA, Klareskog L, Ouchterlony O (1988) Reverse ELISPOT assay for clonal analysis of cytokine production. I. Enumeration of gamma-interferon-secreting cells. *J Immunol Methods* 110 (1):29–36:29. [https://doi.org/10.1016/0022-1759\(88\)90079-8](https://doi.org/10.1016/0022-1759(88)90079-8)
28. Forsthuber T, Yip HC, Lehmann PV (1996) Induction of TH1 and TH2 immunity in neonatal mice. *Science* 271(5256):1728–1730. <https://doi.org/10.1126/science.271.5256.1728>
29. Lehmann PV (1995) Methods for measuring T-cell cytokines United States Patent 6410252
30. Fecher P, Caspell R, Nacem V, Karulin AY, Kuerten S, Lehmann PV (2018) B cells and B cell blasts withstand cryopreservation while retaining their functionality for producing antibody. *Cell* 7(6). <https://doi.org/10.3390/cells7060050>
31. Bisceglia H, Barrier J, Ruiz J, Pagnon A (2023) A FluoroSpot B assay for the detection of IgA and IgG SARS-CoV-2 spike-specific memory B cells: optimization and qualification for use in COVID-19 vaccine trials. *J Immunol Methods* 515:113457. <https://doi.org/10.1016/j.jim.2023.113457>
32. Morell A, Terry WD, Waldmann TA (1970) Metabolic properties of IgG subclasses in man. *J Clin Invest* 49(4):673–680. <https://doi.org/10.1172/JCI106279>
33. Blandino R, Baumgarth N (2019) Secreted IgM: new tricks for an old molecule. *J Leukoc Biol* 106(5):1021–1034. <https://doi.org/10.1002/JLB.3RI0519-161R>
34. van Tetering G, Evers M, Chan C, Stip M, Leusen J (2020) Fc engineering strategies to advance IgA antibodies as therapeutic agents. *Antibodies (Basel)* 9(4). <https://doi.org/10.3390/antib9040070>
35. Normansell R, Walker S, Milan SJ, Walters EH, Nair P (2014) Omalizumab for asthma in adults and children. *Cochrane Database Syst Rev* 1:CD003559. <https://doi.org/10.1002/14651858.CD003559.pub4>
36. Ardeniz O, Unger S, Onay H, Ammann S, Keck C, Cianga C, Gerceker B, Martin B, Fuchs I, Salzer U, Ikinogullari A, Guloglu D, Dereli T, Thimme R, Ehl S, Schwarz K, Schmitt-Graeff A, Cianga P, Fisch P, Warnatz K (2015) beta2-microglobulin deficiency causes a complex immunodeficiency of the innate and adaptive immune system. *J Allergy Clin Immunol* 136(2):392–401. <https://doi.org/10.1016/j.jaci.2014.12.1937>
37. Stapleton NM, Andersen JT, Stemerding AM, Bjarnarson SP, Verheul RC, Gerritsen J, Zhao Y, Kleijer M, Sandlie I, de Haas M, Jonsdottir I, van der Schoot CE, Vidarsson G (2011) Competition for FcRn-mediated transport gives rise to short half-life of human IgG3 and offers therapeutic potential. *Nat Commun* 2:599. <https://doi.org/10.1038/ncomms1608>
38. Bruhns P, Jonsson F (2015) Mouse and human FcR effector functions. *Immunol Rev* 268(1): 25–51. <https://doi.org/10.1111/imr.12350>
39. Weskamm LM, Dahlke C, Addo MM (2022) Flow cytometric protocol to characterize human memory B cells directed against SARS-CoV-2 spike protein antigens. *STAR Protoc* 3(4):101902. <https://doi.org/10.1016/j.xpro.2022.101902>
40. Fryer HA, Hartley GE, Edwards ESJ, Varese N, Boo I, Bornheimer SJ, Hogarth PM, Drummer HE, O’Hehir RE, van Zelm MC (2023) COVID-19 adenoviral vector vaccination elicits a robust memory B cell response with the capacity to recognize omicron BA.2 and BA.5 variants. *J Clin Immunol* 43:1506. <https://doi.org/10.1007/s10875-023-01527-2>
41. Franke F, Kirchenbaum GA, Kuerten S, Lehmann PV (2020) IL-21 in conjunction with anti-CD40 and IL-4 constitutes a potent polyclonal B cell stimulator for monitoring antigen-specific memory B cells. *Cells* 9(2). <https://doi.org/10.3390/cells9020433>

42. Saunders SP, Ma EGM, Aranda CJ, Curotto de Lafaille MA (2019) Non-classical B cell memory of allergic IgE responses. *Front Immunol* 10:715. <https://doi.org/10.3389/fimmu.2019.00715>
43. Phelps A, Bruton K, Grydziuszko E, Koenig JFE, Jordana M (2022) The road toward transformative treatments for food allergy. *Front Allergy* 3:826623. <https://doi.org/10.3389/falgy.2022.826623>
44. Weiss AJ (2012) Overview of membranes and membrane plates used in research and diagnostic ELISPOT assays. *Methods Mol Biol* 792: 243–256. [https://doi.org/10.1007/978-1-61779-325-7\\_19](https://doi.org/10.1007/978-1-61779-325-7_19)
45. Lehmann PV, Lehmann AA (2020) Aleatory epitope recognition prevails in human T cell responses? *Crit Rev Immunol* 40(3):225–235. <https://doi.org/10.1615/CritRevImmunol.2020034838>
46. Karulin AY, Karacsony K, Zhang W, Targoni OS, Moldovan I, Dittrich M, Sundararaman S, Lehmann PV (2015) ELISPOTs produced by CD8 and CD4 cells follow log normal size distribution permitting objective counting. *Cell* 4(1):56–70. <https://doi.org/10.3390/cells4010056>
47. Sundararaman S, Karulin AY, Ansari T, BenHamouda N, Gottwein J, Laxmanan S, Levine SM, Loffredo JT, McArdle S, Neudoerfl C, Roen D, Silina K, Welch M, Lehmann PV (2015) High reproducibility of ELISPOT counts from nine different laboratories. *Cell* 4(1):21–39. <https://doi.org/10.3390/cells4010021>

**Open Access** This chapter is licensed under the terms of the Creative Commons Attribution 4.0 International License (<http://creativecommons.org/licenses/by/4.0/>), which permits use, sharing, adaptation, distribution and reproduction in any medium or format, as long as you give appropriate credit to the original author(s) and the source, provide a link to the Creative Commons license and indicate if changes were made.

The images or other third party material in this chapter are included in the chapter's Creative Commons license, unless indicated otherwise in a credit line to the material. If material is not included in the chapter's Creative Commons license and your intended use is not permitted by statutory regulation or exceeds the permitted use, you will need to obtain permission directly from the copyright holder.

